The Crystal Structure of Zinc-Containing Ferredoxin from the Thermoacidophilic Archaeon *Sulfolobus* sp. Strain 7[†,‡]

Tomomi Fujii,*[,§] Yasuo Hata,[§] Masato Oozeki,[||] Hideaki Moriyama,[||] Takayoshi Wakagi,[||,⊥] Nobuo Tanaka,[||] and Tairo Oshima[||,#]

Institute for Chemical Research, Kyoto University, Uji, Kyoto 611, Japan, and Department of Life Science, Faculty of Bioscience and Biotechnology, Tokyo Institute of Technology, Nagatsuta, Yokohama, Kanagawa 226, Japan

Received August 6, 1996; Revised Manuscript Received November 22, 1996[⊗]

ABSTRACT: The crystal structure of ferredoxin from the thermoacidophilic archaeon *Sulfolobus* sp. strain 7 was determined by multiple isomorphous replacement supplemented with anomalous scattering effects of iron atoms in the Fe-S clusters, and refined at 2.0 Å resolution to a crystallographic *R* value of 0.173. The structural model contains a polypeptide chain of 103 amino acid residues, 2 [3Fe-4S] clusters, and 31 water molecules; in this model, the cluster corresponding to cluster II in bacterial dicluster ferredoxins loses the fourth iron atom although it may originally be a [4Fe-4S] cluster. The structure of the archaeal ferredoxin consists of two parts: the core fold part (residues 37−103) and the N-terminal extension part (residues 1−36). The "core fold" part has an overall main-chain folding common to bacterial dicluster ferredoxins, containing two clusters as the active center, two α-helices near the clusters, and two sheets of two-stranded antiparallel β-sheet (the terminal and central β-sheets). The "N-terminal extension" part is mainly formed by a one-turn α-helix and a three-stranded antiparallel β-sheet. The β-sheet in the N-terminal extension is hydrogen-bonded with the terminal β-sheet in the core fold to form a larger β-sheet. The distinct structural feature of this archaeal ferredoxin lies in the zinc-binding center where the zinc ion is tetrahedrally ligated by four amino acid residues (His 16, His 19, and His 34 from the N-terminal extension, and Asp 76 from the core fold). The zinc ion in the zinc-binding center is located at the interface between the core fold and the N-terminal extension, and connects the β-sheet in the N-terminal extension and the central β-sheet in the core fold through the zinc ligation. Thus, the zinc ion plays an important role in stabilizing the structure of the present archaeal ferredoxin by connecting the N-terminal extension and the core fold, which may be common to thermoacidophilic archaeal ferredoxins.

Archaea (archaebacteria), which grow under extreme conditions such as high temperature, strong acidity, high salinity, and anaerobicity, constitute a group of organisms which is distinct from Bacteria and Eucarya (Woese et al., 1990). In the course of evolution, they have adapted to such very harsh environments by evolving their special adaptation mechanisms. It is, therefore, of interest to investigate the mechanisms of their biological adaptation to extreme environments on the molecular level. Arousing interests not only in their evolutionary status but also in the stabilization mechanism of proteins they produce under such extreme environments, our studies on archaeal ferredoxins have been carried out from biochemical and biophysical points of view.

Ferredoxins (Fds)[1] are distributed over a wide range of living organisms from archaea to humans. Various kinds of Fds isolated from different organisms have been studied biochemically and biophysically, and are classified by the geometry of the Fe-S cluster into two types: the plant-type Fds and the bacterial-type Fds (Bruschi & Guerlesquin, 1988; Knaff & Hirasawa, 1991). Plant-type Fds are characterized not only by a single [2Fe-2S] cluster but also by a unique protein fold consisting of a four-stranded mixed β-sheet, an α-helix, and a long loop containing three of four cysteine ligands to the iron atoms. Ferredoxins of this type have also been isolated from archaea and vertebrates. A recent X-ray analysis of a 2Fe-2S ferredoxin from a halophilic archaeon, *Haloarcula marismortui*, has revealed that the ferredoxin has a protein folding similar to those of plant-type Fds although its insertion of 30 residues forms an extra domain made up of 2 amphipathic helices and intervening loops (Frolow et al., 1996).

Bacterial-type Fds have many variants which differ in the number of clusters (one or two), the type of cluster ([4Fe-4S] or [3Fe-4S]), and the length of polypeptide chain (insertion or terminal extension). Three-dimensional structures of several bacterial Fds have been elucidated by X-ray analysis (Adman et al., 1976; Fukuyama et al., 1989; Stout, 1989; Kissinger et al., 1991; Séry et al., 1994; Duée et al., 1994). On the basis of their structural features, the probable evolutionary process of bacterial Fds was discussed by

[†]This research was supported in part by Grants-in-Aid for Scientific Research (9200417 to T.F.) and for Scientific Research on Priority Areas (08249220 to Y.H.) from The Ministry of Education, Science, Sports and Culture of Japan, and by the Sakabe project of the TARA (Tsukuba Advanced Research Alliance) center at the University of Tsukuba.

[‡] The coordinates have been deposited in the Brookhaven Protein Data Bank (file name 1XER).

* To whom correspondence should be addressed.

[§] Kyoto University.

[||] Tokyo Institute of Technology.

[⊥] Present address: Department of Biotechnology, The University of Tokyo, 1-1-1 Yayoi, Bunkyo-ku, Tokyo 113, Japan.

[#] Present address: Department of Molecular Biology, Tokyo University of Pharmacy and Life Science, Horinouchi, Hachioji, Tokyo 192-03, Japan.

[⊗] Abstract published in *Advance ACS Abstracts,* January 15, 1997.

[1] Abbreviation: Fd; ferredoxin.

S0006-2960(96)01966-6 CCC: $14.00

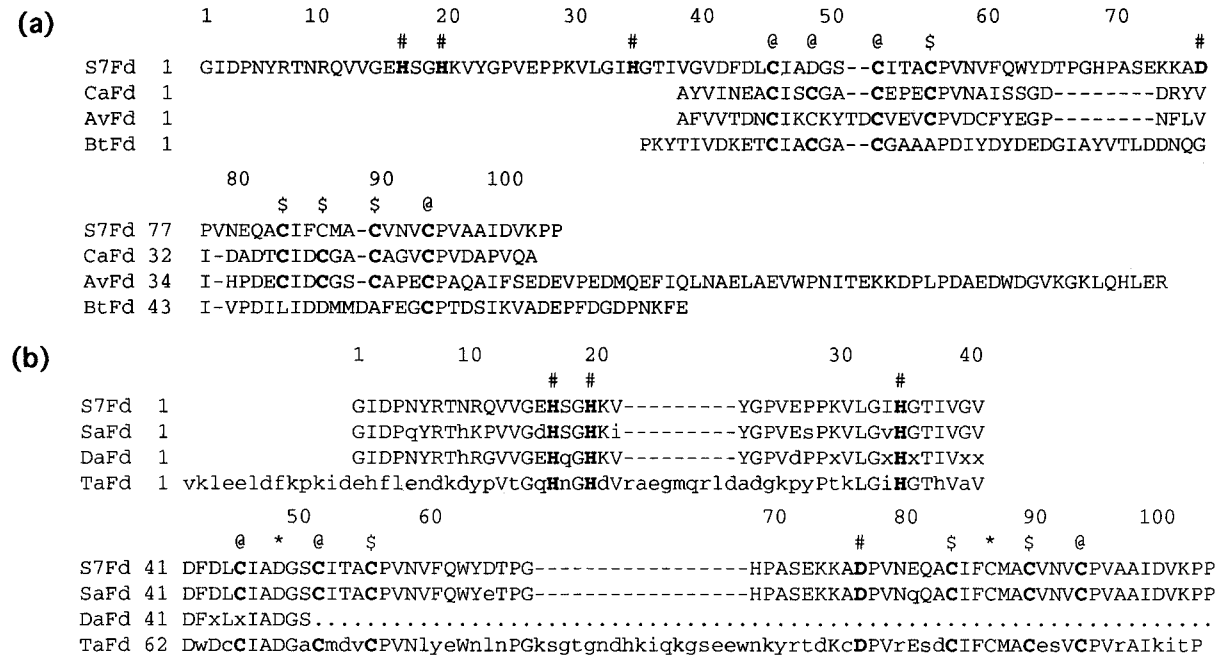

FIGURE 1: (a) Sequence alignment of bacterial Fds based on their tertiary structures. S7Fd is *Sulfolobus* sp. strain 7 Fd (N-terminal protrusion type); CaFd is *Clostridium acidurici* Fd (common core fold type); AvFd is *Azotobacter vinelandii* Fd I (C-terminal protrusion type); BtFd is *Bacillus thermoproteolyticus* Fd (monocluster and insertion type). The numbering refers to the S7Fd sequence. The residues shown in bold type are the ligating ones for Fe-S clusters or the important ones referred to in the text. The cysteine residues ligating Fe-S clusters I and II are marked with @ and $, respectively. The residues ligating the zinc ion in S7Fd are marked with #. (b) Sequence alignment of thermoacidophilic archaeal Fds. S7Fd is *Sulfolobus* sp. strain 7 Fd; SaFd is *Sulfolobus acidocaldarius* Fd; DaFd is *Desulfurolobus ambivalens* Fd; TaFd is *Thermoplasma acidophilum* Fd. The numbering refers to the S7Fd sequence. Capital letters denote identical residues with S7Fd sequence. The residues shown in bold type are ligating ones for the Fe-S cluster or zinc atom. The cysteine residues ligating Fe-S clusters I and II in S7Fd are marked with @ and $, respectively. The residues ligating the zinc ion in S7Fd are marked with #. The residues Asp 48 and Cys 86 of S7Fd are indicated with *. The sequence of DaFd is reported for only the N-terminal half.

Fukuyama et al. (1988). The dicluster-type bacterial Fds including 2 [4Fe-4S] Fds and [3Fe-4S][4Fe-4S] Fds share a common protein fold known as the $(\beta\alpha\beta)_2$ fold, which ligates two cubane-like Fe-S clusters and has an intramolecular pseudo-2-fold symmetry (Adman et al., 1976; Duée et al., 1994). These structural features imply that the dicluster-type bacterial Fds evolved from a common ancestor after gene duplication. The monocluster-type bacterial Fds have a $(\beta\alpha\beta)_2$ fold similar to that of the dicluster-type bacterial Fds. In the monocluster-type Fds, the second cluster of dicluster-type Fds is deleted, and the second α-helix is elongated to the characteristic α-helix of monocluster-type Fds which fills up the space of the second cluster. These structural features have been deduced from studies of eubacterial Fds.

During the last decade, several bacterial-type Fds have been isolated and purified from archaea of hyperthermophiles, methanogens, and thermoacidophiles. They have been classified into three types by both the polypeptide chain length and the type of Fe-S cluster; Fds from hyperthermophiles, methanogens, and thermoacidophiles are characterized as the monocluster type, the dicluster type, and the dicluster type with N-terminal extended region, respectively. Of these three types of archaeal Fds, a unique group of ferredoxins with N-terminal extension has been found exclusively from thermoacidophilic archaea (Wakabayashi et al., 1983; Minami et al., 1985; Iwasaki et al., 1994; Teixeira et al., 1995). In spite of intensive studies of archaeal Fds, no three-dimensional structure of bacterial-type Fds from archaea has been elucidated at atomic resolution, although there is a report dealing with ^{1}H NMR determination of the secondary structure of ferredoxin from the hyperthermophilic archaeon *Pyrococcus furiosus* (Teng et al., 1994). Studies on tertiary structures of thermoacidophilic archaeal Fds may shed light on the stabilization mechanism and the evolutionary status of archaeal Fds.

Sulfolobus sp. strain 7 is a thermoacidophilic archaeon which grows optimally at pH 2.5−3.0 and 75−80 °C (Wakagi & Oshima, 1985). The archaeon acquires biological energy by aerobic respiration rather than simple fermentation. Ferredoxin from *Sulfolobus* sp. strain 7 is known to serve as an electron acceptor of a 2-oxoacid:Fd oxidoreductase (Iwasaki et al., 1994, 1995; Kerscher et al., 1982). The *Sulfolobus* Fd is a bacterial dicluster-type Fd (Iwasaki et al., 1994). From studies of electron paramagnetic resonance (EPR) and cyclic voltammetry, the clusters in this ferredoxin were assigned to the [3Fe-4S] (cluster I) and [4Fe-4S] (cluster II) clusters, with midpoint redox potentials of −280 and −530 mV, respectively (Iwasaki et al., 1994). It has been demonstrated that cluster I plays a redox role, whereas cluster II apparently plays a structural role. The *Sulfolobus* Fd molecule consists of a polypeptide of 103 amino acid residues (Wakagi et al., 1996), and its primary structure is distinct from those of bacterial Fds in 2 regions; the *Sulfolobus* Fd has an N-terminal extension of about 40 residues and an insertion of about 10 residues in the middle of the polypeptide chain (Figure 1). Such a characteristic extension and insertion in sequence has also been found in ferredoxins from thermoacidophilic archaea such as *Sulfolobus acidocaldarius* (Minami et al., 1985; Breton et al., 1995), *Desulfurolobus ambivalens* (Teixeira et al., 1995), and *Thermoplasma acidophilum* (Wakabayashi et al., 1983). Therefore, the additional regions are expected to adopt informative conformations characteristic to thermoacidophilic archaeal Fds.

In this paper, we report the 2.0 Å resolution crystal structure of ferredoxin from *Sulfolobus* sp. strain 7, which is a unique zinc-ligating ferredoxin, and we discuss the importance of the zinc-binding center in stabilizing archaeal Fds by comparing the present structure with those of other bacterial Fds.

MATERIALS AND METHODS

Crystal Preparation and Data Collection. The ferredoxin was isolated from a thermoacidophile, *Sulfolobus* sp. strain 7, which is identical to the *S. acidocaldarius* strain 7 designated previously (Fujii et al., 1991), and different from both *S. acidocaldarius* DSM639 and *S. solfataricus* DSM 1616 as judged from the 16S rDNA sequence (Oshima et al., unpublished observation). All procedures for purification and crystallization were carried out under aerobic conditions. The *Sulfolobus* Fd was crystallized by a batch method. Fine-powdered ammonium sulfate was slowly added to 300 μL of 5 mg/mL protein solution (0.5M Tris/maleate/NaOH buffer, 1% 2-methyl-2,4-pentanediol, pH 5.0) until the solution became slightly turbid (1.9−2.1 M). The crystallization solution was stored at 37 °C in an incubator. Dark brown crystals with approximate dimensions of 0.3 × 0.3 × 0.5 mm were obtained in 3−5 weeks. To enhance the reproducibility in the subsequent crystallization, a drop of the mother liquor containing a small number of microcrystals was added to the crystallization solution just before the crystallization began. The crystals obtained in this way belong to the tetragonal space group $P4_32_12$ with cell dimensions of $a = b = 50.12$ Å and $c = 69.52$ Å, and contain one Fd molecule per asymmetric unit. The absolute configuration was fixed by a Bijvoet-difference Fourier map showing the appearance of positive peaks for the Fe-S clusters, as described below.

For phasing by the isomorphous replacement method, two kinds of heavy-atom derivative crystals were prepared by soaking native crystals in 3.0 M $(NH_4)_2SO_4$ solutions containing 50 mM $UO_2(NO_3)_2$ and 100 mM $K_2Pt(CN)_4$ for 3 days and 21 h, respectively. Diffraction data for the native and two derivative crystals were collected at room temperature on an R-AXIS IIC imaging plate system, using CuKα radiation monochromatized with Supper double-focusing mirrors installed on a Rigaku RU200 rotating anode X-ray generator operated at 40 kV and 100 mA. The crystals were mounted with the c^* axis along the spindle axis in order to record mirror-related Bijvoet mates on the same frame. Data processing was accomplished using the R-AXIS software package. X-ray data collection statistics are summarized in Table 1.

Structure Determination and Refinement. The structure was determined by the isomorphous replacement method for the uranium and platinum derivatives, supplemented with anomalous dispersion effects from the iron atoms of the Fe-S clusters as well as the uranium atoms in the derivative. Calculations for phasing were carried out with the program package PHASES (Furey & Swaminathan, 1990). The iron atoms in the clusters were located with Bijvoet-difference Fourier maps for the native crystal. A Bijvoet-difference Fourier map for the native crystal at 5.0 Å resolution revealed two large positive density peaks with about 12 Å separation from each other, which correspond to two Fe-S clusters. The Bijvoet-difference Fourier map, calculated with Bijvoet-difference amplitudes of the native crystal and isomorphous replacement phases, was used to fix the absolute configuration. The correct Fourier map showed the appearance of positive peaks for the Fe-S clusters. As the resolution of the map was increased to 2.0 Å, each of the large peaks was resolved into three small peaks which were separated by 2.7 Å from one another (Figure 2). The geometrical relationships among these peaks were similar to those of iron atoms for the [3Fe-4S] cluster in *Azotobacter vinelandii* Fd I and *Desulfovibrio gigas* Fd II (Stout, 1989; Kissinger et al., 1991). These six small peaks were interpreted to be iron atoms in the clusters, and the anomalous scattering effects of the iron atoms against CuKα radiation were included in phase calculation. Solvent-flattening procedures were undertaken to improve the quality of the density map. The mask map was made with a sphere of radius 7.5 Å and an estimated 25% solvent content (Wang, 1985). The electron density maps calculated before and after solvent-flattening modification were used for model building of the present Fd.

Table 1: Statistics for Data Collection and Phase Calculation

	native	$UO_2(NO_3)_2$	$K_2Pt(CN)_4$
data collection			
resolution limit (Å)	1.7	1.8	2.0
obsd reflections	29180	24441	19996
independent reflections	8687	7538	5811
completeness[a] (%)	86.0 (89.9)	86.3 (89.0)	89.6 (89.6)
R_{merge}[b]	6.19	9.50	8.04
MIR analysis (2.0 Å)			
no. of sites		2	2
phasing power[c]		1.72	1.18
mean FOM[d] (MIR+AS[e])	0.637		
mean FOM (solvent flattening)	0.898		

[a] The values at 2.0 Å resolution are given in parentheses. [b] $R_{merge} = \sum_i|\langle I_i\rangle - I_i|/\sum_i I_i$, where $\langle I_i\rangle$ is average of I_i over all symmetry equivalents. [c] Phasing power $= \langle F_H\rangle/\langle E\rangle$, where $\langle F_H\rangle$ is the rms calculated heavy atom structure factor amplitude and $\langle E\rangle$ is the rms lack of closure error. [d] FOM is the figure of merit. [e] MIR+AS is the multiple isomorphous replacement method supplemented with anomalous scattering effects.

The model of the Fd molecule was built on the computer graphics IRIS-Indigo Elan with the program Turbo-FRODO (Cambillau, 1992). The interpretation of the maps was straightforward in most parts, especially around the [3Fe-4S] cluster (cluster I). However, the density maps were unclear in the vicinity of the other cluster (cluster II). Therefore, the poor density region was interpreted using the structure of *P. aerogenes* Fd as a guide. Despite the complete interpretation of the densities corresponding to the polypeptide chain and the Fe-S clusters, there was one high density peak left uninterpreted in the inside of the molecule. This peak was estimated to be a metal ion because three histidine and one aspartate residues were arranged tetrahedrally around the peak (Figure 3a). However, the peak was still left uninterpreted at this stage.

The model was refined with the molecular dynamics program X-PLOR using a slow-cool protocol (from 3000 K to 300 K) (Brünger, 1992a). About 10% of the observed reflections were randomly selected and set aside for cross-validation analysis (Brünger, 1992b). The $2F_o - F_c$ and $F_o - F_c$ maps were used to correct the model every refinement cycle. After the R factor was reduced to 0.266, a total of 31 water molecules were added to the model to be refined, and then the temperature factors of all atoms were refined

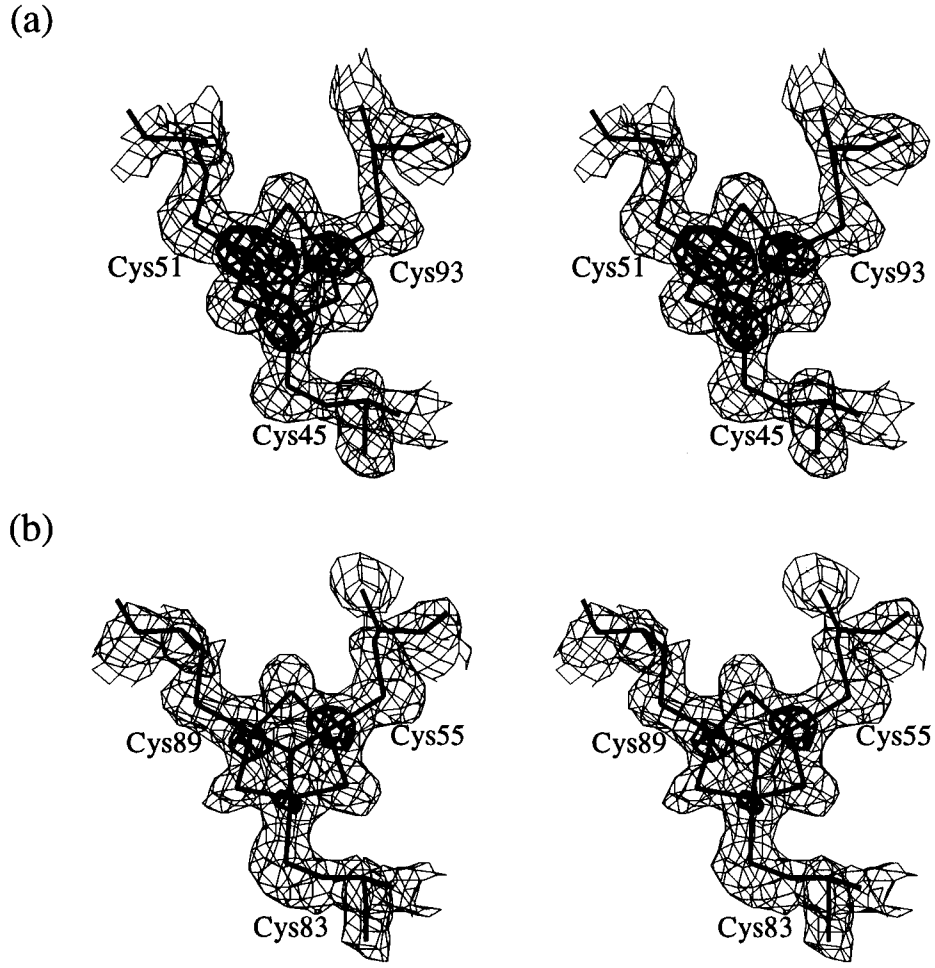

FIGURE 2: Fe-S clusters of the *Sulfolobus* Fd. The electron density ($2F_o - F_c$) map at 2.0 Å resolution is shown in a thin line and contoured at the 1σ level. The Bijvoet-difference Fourier map at 2.0 Å resolution is shown in a thick line and contoured at the 5σ level. The wire models of the [3Fe-4S] clusters and ligand cysteines are superimposed on the maps: (a) cluster I and (b) cluster II.

up to an *R* factor of 0.191. However, an $F_o - F_c$ map still showed a high positive peak which was larger than the 20σ contour level. This peak, which was tetrahedrally coordinated by four amino acid residues of His 16, His 19, His 34, and Asp 78, was attributed to a divalent metal cation such as Zn^{2+}. The X-ray crystallographic identification of the metal ion was performed using anomalous dispersion effects characteristic for zinc which were measured with a tuneable synchrotron radiation source (Fujii et al., 1996). Finally, the whole model of the Fd molecule was refined to an *R* factor of 0.173 at 2.0 Å resolution.

Quality of the Model. At present, the refinement of the structure model consisting of 103 amino acid residues, 2 [3Fe-4S] clusters, 1 zinc ion, and 31 water molecules has resulted in residuals of $R = 0.173$ and $R_{free} = 0.244$ for 5008 independent reflections ($F > 2\sigma_F$) within 8.0−2.0 Å resolution and randomly selected 608 reflections, respectively. The rms deviations from ideal bond lengths and bond angles are 0.011 Å and 1.768°, respectively. The polypeptide dihedral angles (ϕ, ψ) for most non-glycine residues (83.1%) fall in the most favored regions (Laskowski, 1993). The average temperature factors for the main-chain atoms and the side-chain atoms are 14.0 and 15.5 Å^2, respectively. Residues ranging from 85 to 91 and from 101 to 103 (C-terminus) have large average temperature factors (>30.0 Å^2). The average temperature factors for clusters I and II are 10.9 and 24.0 Å^2, respectively.

RESULTS

Overall Topology. The overall structure of the *Sulfolobus* Fd molecule is depicted in Figure 4. The molecule has an ellipsoidal shape with an approximate size of 30 Å × 30 Å × 35 Å. It has secondary structures of three α-helices, one 3_{10}-helix, seven β-strands, and eight turns. The protein folding of the *Sulfolobus* Fd can be divided into two parts by a structural comparison of the present archaeal Fd with other bacterial dicluster Fds (Figure 5). One is the "core fold" part (residues 37−103), which binds two [3Fe-4S] clusters and has a topologically conserved protein folding, a $(\beta\alpha\beta)_2$ fold, common to bacterial dicluster Fds. The rms deviation in corresponding Cα atoms between the core fold of the *Sulfolobus* Fd and *Clostridium acidurici* Fd is 1.8 Å. The other is the "N-terminal extension" part (residues 1−36), which is mainly formed by three β-strands. The N-terminal extension has two *cis*-proline residues at positions 24 and 28 of the polypeptide chain. Interestingly, the *Sulfolobus* Fd molecule contains the zinc-binding center which is located at the interface between the core fold and the N-terminal extension (Figures 4 and 5a). The zinc ion is tetrahedrally ligated by four amino acid residues, three of which come from the N-terminal extension and the last from the core fold. The distance between the centers of the clusters is 12.0 Å, and the distances between the zinc ion and cluster I or cluster II are 13.3 and 15.4 Å, respectively.

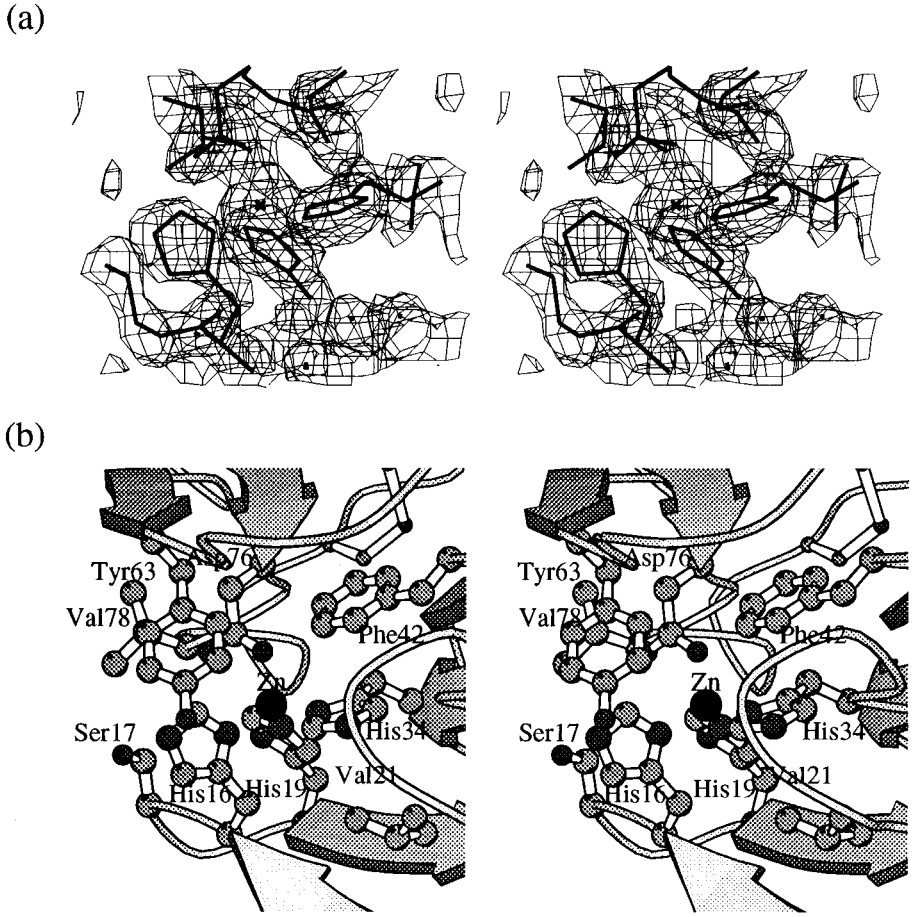

FIGURE 3: Zinc-binding center in the *Sulfolobus* Fd. (a) The $2F_o - F_c$ map at 2.0 Å resolution is shown in a thin line and contoured at the 1σ level. The wire models of four ligand and the surrounding residues for the zinc ion are superimposed on the maps. (b) Schematic drawing of the zinc-binding site. Zn ligands and the surrounding residues are depicted with a ball-and-stick model. The view of the figure is similar to that of (a). This figure was generated using the program MOLSCRIPT (Kraulis, 1991).

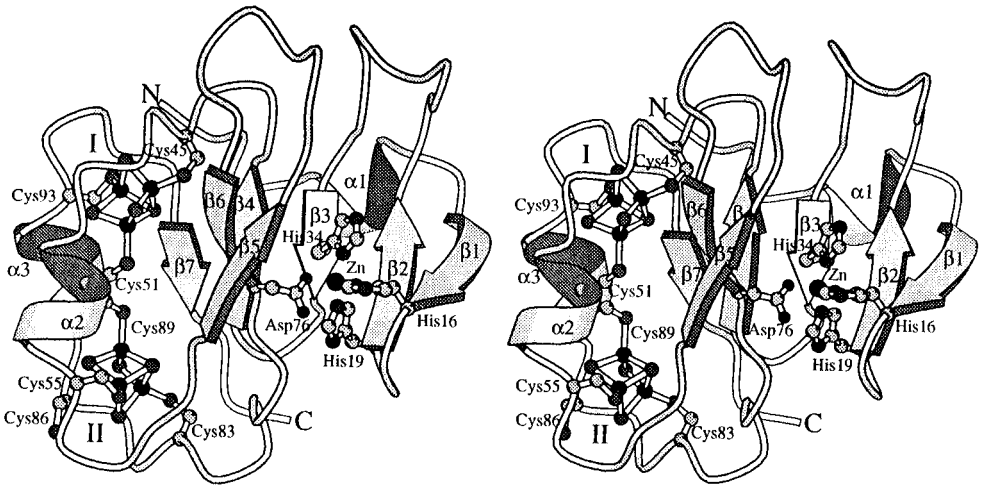

FIGURE 4: Schematic drawing of the *Sulfolobus* Fd molecule. β-Strands are shown as gray arrows, and α-helices are shown as gray ribbons. The [3Fe-4S] clusters, the seven cysteines, the zinc ion, and the four zinc-ligand residues are represented as ball-and-stick models: light gray balls for carbons, dark gray small balls for oxygens, dark gray middle size balls for nitrogens, light gray middle size balls for sulfurs, black middle size balls for irons, and black large ball for zinc. Fe-S clusters I and II are indicated as I and II, respectively. This figure was generated using the program MOLSCRIPT (Kraulis, 1991).

Core Fold Ligating Fe-S Clusters. The core fold ligating two [3Fe-4S] clusters has a $(\beta\alpha\beta)_2$ protein fold and an intramolecular 2-fold axis roughly relating the N-terminal half to the C-terminal half. The clusters are sandwiched by two α-helices, α2 (residues 50−54) and α3 (residues 88−92), and two double-stranded β-sheets, antiparallel β-sheet A composed of β4 (residues 38−41) and β7 (residues 98−100) and antiparallel β-sheet B of β5 (residues 61−64) and β6 (residues 73−76); besides, the top of cluster I and the bottom of cluster II are located near the surface (Figure 4). This type of protein folding of the core fold is common to bacterial dicluster Fds. The major conformational differences between the core fold of the *Sulfolobus* Fd and other bacterial Fds lie in the region of residues 80−82 and the insertion of

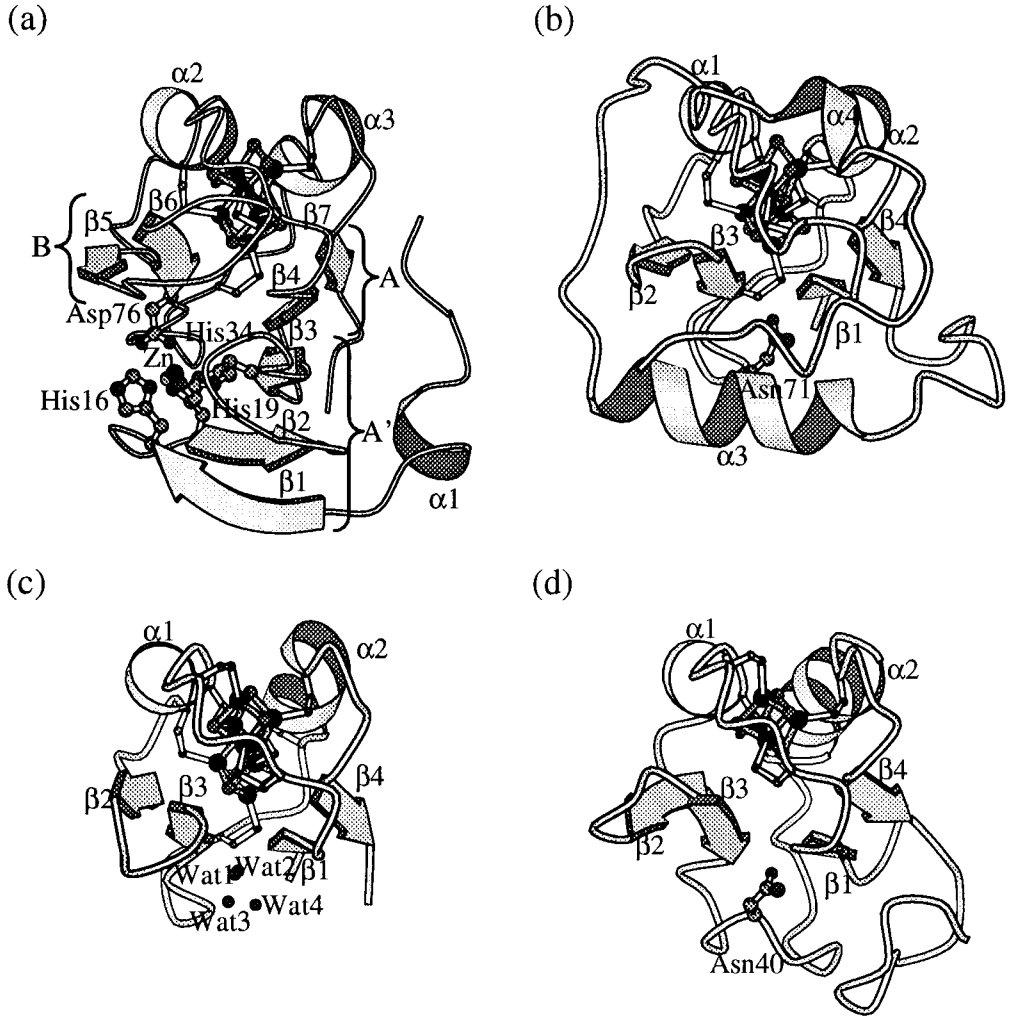

FIGURE 5: Schematic drawing of the *Sulfolobus* Fd and several bacterial Fd molecules, viewed from the top of Figure 4. (a) The *Sulfolobus* Fd, (b) *Azotobacter vinelandii* Fd I, (c) *Clostridium acidurici* Fd, and (d) *Bacillus thermoproteolyticus* Fd. The Fe-S clusters and the residues which participate in interaction between β-sheets A and B are represented with ball-and-stick models: light gray balls for carbons, dark gray small balls for oxygens, dark gray middle size balls for nitrogens, light gray middle size balls for sulfurs, black middle size balls for irons, and black large ball for zinc. The atoms of the Fe-S cluster ligating cysteine residues are only represented with small balls. β-Sheets A (strands β4 and β7), A′ (strands β1, β2, and β3), and B (strands β5 and β6) in the *Sulfolobus* Fd are indicated as A, A′, and B, respectively. The figures were generated using the program MOLSCRIPT (Kraulis, 1991).

residues 65−72 (8 residues) in the present Fd (Figure 1a). The region of residues 80−82 has a 3_{10}-helix conformation, although the corresponding region of other bacterial Fds has a turn conformation. The insertion ranging from Thr 65 to Glu 72 adopts a loop structure. The loop is inserted between strands β5 and β6 which form antiparallel β-sheet B, and elongates the original loop connecting both the strands. The elongated loop contains two proline residues (Pro 66 and Pro 69) and three hydrogen bonds within the loop interior. Consequently, the inserted region seems to have a relatively stable loop structure for its length. The side chain of His 68 in the insertion loop makes a hydrogen bond with the side chain of Asp 43 in the loop between strand β4 and α-helix α2. Moreover, the inserted loop in the core fold is located close to the loop between strands β2 and β3 in the N-terminal extension. The hydrogen bond between the main-chain carbonyl O of Gly 67 and the Nζ of Lys 29 may contribute to the interaction between the loops, although the Nζ of Lys 29 is monomethylated (Minami et al., 1985; Wakagi et al., 1996) and the electron density map for the side chain of Lys 29 is not so clear.

The *Sulfolobus* ferredoxin is isolated as a dicluster Fd ligating the [3Fe-4S] and [4Fe-4S] clusters. The geometry of the clusters is essentially similar to that observed in the [3Fe-4S] and [4Fe-4S] clusters of other bacterial Fds (Adman et al., 1976; Fukuyama et al., 1989; Stout, 1989; Kissinger et al., 1991; Séry et al., 1994; Duée et al., 1994); the average Fe-S bond lengths in the present clusters I and II are 2.29 and 2.32 Å, respectively. Cluster I is the [3Fe-4S] cluster ligated by three cysteine residues of Cys 45, Cys 51, and Cys 93. Bacterial dicluster Fds usually have a pair of consensus Fe-S cluster-binding sequences, Cys-X-X-Cys-X-X-Cys-X-X-X-Cys-Pro. However, the N-terminal half of the core fold of the *Sulfolobus* Fd has an incomplete cluster-binding sequence. From an initial comparison of the cluster-binding sequence with other dicluster Fds, Asp 48 in the *Sulfolobus* Fd, which corresponds to the second cysteine residue in the other Fds (Figure 1a), was assumed to be the second ligand for the [4Fe-4S] cluster (Minami et al., 1985). Consequently, the present analysis has shown the assumption to be false for the *Sulfolobus* Fd. In the present structure model, the carboxyl Oδ1 of Asp 48 is rotated away from the Fe-S cluster to make hydrogen bonds with the side-chain Oγ and the main-chain amide NH of Ser 50, which shows that cluster I is the [3Fe-4S] cluster. Around cluster I, the electron density is well-defined (Figure 2a), and the polypep-

tide chain is well-ordered. Consequently, temperature factors of atoms around cluster I are relatively low (about 15 Å^2), and the polypeptide conformation is very stable around the cluster. The existence of cluster I is conserved throughout all the types (monocluster and dicluster types) of bacterial Fds (Iwasaki et al., 1994). In contrast to cluster I, cluster II has a high average temperature factor, and the electron density map is ambiguous in the vicinity of the cluster (Figure 2b). In the present model, cluster II is ligated by three cysteine residues, Cys 55, Cys 83, and Cys 89. Cluster II in dicluster Fds is normally [4Fe-4S] ligated by four cysteine residues (Adman et al., 1976; Stout et al., 1989; Duée et al., 1994). The C-terminal half in the core fold of the *Sulfolobus* Fd has a complete consensus cluster-binding sequence, and Cys 86 corresponding to the second cysteine residue in the present Fd should bind to the iron atom. However, the electron density for Cys 86 is remarkably low, and, moreover, the second iron atom in the cluster does not appear clearly in electron density maps. Even in a Bijvoet-difference Fourier map at 2 Å resolution, there were only three peaks, not four peaks, at the position of cluster II (Figure 2b). Temperature factors for the polypeptide chain around Cys 86 (>30 Å^2) and cluster II (24.0 Å^2 on the average) are very high, although the average of temperature factors for all the atoms is normal (15.0 Å^2) in the present structure. An EPR analysis and a quantitative analysis of iron content show that the present Fd should originally contain a pair of [3Fe-4S] and [4Fe-4S] clusters. These facts indicate that the second iron atom of cluster II in the present Fd crystals has been released from the original [4Fe-4S] cluster for some reason, and that, consequently, the surrounding conformations become unstable. The comparison between the polypeptide conformations of the [3Fe-4S] and [4Fe-4S] clusters observed in other bacterial Fds reveals a local conformational difference between them. In the conformation of the [3Fe-4S] cluster, the Cα atom of the residue corresponding to the second cysteine of the [4Fe-4S] cluster is closer to the cluster by 1.5−2.0 Å than expected (Kissinger et al., 1991). The polypeptide conformation around cluster I in the *Sulfolobus* Fd is very similar to that of the [3Fe-4S] cluster in other Fds (Stout, 1989; Kissinger et al., 1991). However, the polypeptide conformation around cluster II in the *Sulfolobus* Fd is not so similar to that of the [3Fe-4S] or [4Fe-4S] cluster, and is likely to be an intermediate form between the [3Fe-4S] and [4Fe-4S] cluster conformations. This fact may result from the incomplete dissociation of Cys 86 from cluster II. However, it is important to point out the striking similarity between the environment for Cys 86 partially dissociating from cluster II and that for Asp 48 in cluster I, the [3Fe-4S] cluster, because both residues are the second residue in the consensus cluster-binding sequence. In addition, the possibility of interconversion between the [4Fe-4S] and [3Fe-4S] clusters has been reported in ferredoxins I and II from *D. gigas*, which contain a single cluster per subunit in the dimer and tetramer, respectively (Kissinger et al., 1991). This report deals with the interconversion in cluster I. It is not known whether the interconversion could occur in cluster II. The reason for the disruption of cluster II in the *Sulfolobus* Fd remains to be elucidated by further structural studies.

N-Terminal Extension Ligating the Novel Zinc Site. The N-terminal extension mainly consists of a three-stranded antiparallel β-sheet A′ composed of β1 (residues 12−16), β2 (residues 19−22), and β3 (residues 33−34), and one-turn α-helix α1 (residues 6−9) (Figures 4 and 5a). β-Sheet A′ interacts with the terminal β-sheet A (β4 and β7) in the core fold through hydrogen bonds between strands β3 and β4 to form a larger five-stranded β-sheet, A′+A. Interestingly, the N-terminal extension provides the novel zinc-binding site. The zinc ion is in the site located at the interface between the N-terminal extension and the core fold, and is tetrahedrally ligated by four amino acid residues, His 16, His 19, and His 34 from the N-terminal extension and Asp 76 from the core fold (Figures 3, 4, and 5a). The coordinated atoms are Nδ1 of His 16, Nε2 of His 19, Nδ1 of His 34, and Oδ1 of Asp 76. Their coordinate distances are 2.03, 1.92, 1.94, and 1.90 Å, respectively. These values are similar to those observed in structural zinc ions of collagenases (Lovejoy et al., 1994; Spurlino et al., 1994) and superoxide dismutases (Tainer et al., 1982; Kitagawa et al., 1991), which have the same zinc-ligand residues as the present Fd. The zinc ion in the *Sulfolobus* Fd apparently holds the core fold and the N-terminal extension together. It is located about 5 Å deep from the protein surface, and shielded from solvent by the residues His 16, Ser 17, and Tyr 63 (Figure 3b).

DISCUSSION

Unique Structure of Thermoacidophilic Fds. Ferredoxins so far isolated from thermoacidophilic archaea were reported to have the N-terminal extension and insertion, compared with other bacterial Fds (Figure 1). In spite of the difference in the degree of extension and insertion, their amino acid sequences are well conserved around the zinc-binding site (Figure 1b). Two regions corresponding to Val 12−Gly 23 and Val 30−Val 38 in the *Sulfolobus* Fd contain three zinc-ligand histidine residues. The sequence alignment among thermoacidophilic archaeal Fds on the basis of the conserved zinc-ligand residues shows high sequence identity in the regions around the zinc ligands. The total sequence identity in these regions between Fds from *Sulfolobus* sp. strain 7 and *S. acidocaldarius*, *D. ambivalens*, or *T. acidophilum* is 86%, 86%, and 57%, respectively. The high sequence identity allows us to predict that thermoacidophilic archaeal Fds may have the conserved zinc-binding center where the zinc ion is ligated in a similar type of ligation. Of four zinc-ligands in the *Sulfolobus* Fd, three ligands, His 16, His 19, and His 34, are located at the C-, N-, and C-terminal ends of three β-strands, β1−β3, respectively, in the extended N-terminal antiparallel β-sheet A′ which is joined to β-sheet A in the core fold through hydrogen bonds between β3 and β4. Consequently, the zinc ion binds tightly to the larger β-sheet, A′+A, through the Zn−His coordinate bonds. In addition, Asp 76 ligands to the zinc from the C-terminal end of strand β6 in β-sheet B in the core fold. In this way, two β-sheets, A and B, in the core fold, are indirectly linked together by both the zinc ligation and the hydrogen bonds (Figure 5a). The sequence identity observed not only around the zinc-binding center but also in the N-terminal extension, together with the structural similarity in the core fold, suggests that the unique polypeptide folding of the *Sulfolobus* Fd could be common to thermoacidophilic archaeal Fds. The zinc-containing ferredoxin structure observed in the *Sulfolobus* Fd may be characteristic of thermoacidophilic archaeal Fds. In order to make sure of the suggestion, more structures of archaeal Fds should be elucidated, because the present

ferredoxin is the first example of zinc-binding ferredoxin whose tertiary structure has been determined at atomic resolution.

Comparison with Other Bacterial Fds. The core fold of bacterial dicluster Fds has the $(\beta\alpha\beta)_2$ fold where β-sheets A and B are usually so apart from each other that they do not interact directly. In the *Sulfolobus* Fd, as described above, the β-sheets interact indirectly with each other through both the hydrogen bonds between β-sheets A and A′ and the zinc ligation between β-sheets A′ and B. Since the zinc-binding center and β-sheet A′ in the N-terminal extension may be conserved in thermoacidophilic archaeal Fds, the indirect interactions between β-sheets A and B are expected to be observed in other thermoacidophilic archaeal Fds; the indirect interaction in the core fold may be a reasonable way to stabilize the core fold in the dicluster ferredoxin molecule. From this point of view, the inspection of three-dimensional structures of bacterial Fds reveals some interesting information on indirect interaction between the two β-sheets, A and B, in the core fold of the ferredoxins. The [3Fe-4S][4Fe-4S] dicluster ferredoxin I from *A. vinelandii* has a C-terminal extension containing an α-helix. The extended parts of the *Sulfolobus* and *A. vinelandii* Fds are located on the opposite sides of the cluster sites, respectively (Figure 5a,b). Superposition of the Fd structures reveals that the α-helix, the main secondary structure element in the C-terminal extended part of *A. vinelandii* Fd I, roughly overlaps with the zinc-binding site of the *Sulfolobus* Fd. The side-chain nitrogen and oxygen of Asn 71 in the middle of the α-helix in *A. vinelandii* Fd I make hydrogen bonds with main-chain oxygen and nitrogens of β-strands from β-sheets A and B, respectively. As a consequence, the β-sheets are linked together indirectly by the hydrogen-bonding bridge of Asn 71. In the dicluster Fd from *C. acidurici*, several water molecules lie between these β-sheets to bridge them together through hydrogen bonds to amino nitrogens and carbonyl oxygens of the polypeptide backbone (Duée, 1994) (Figure 5c). Even in the monocluster-type Fd from *Bacillus thermoproteolyticus*, the side chain of Asn 40 on an insertion loop makes hydrogen bonds with backbones of β-strands from both β-sheets A and B (Fukuyama et al., 1988) (Figure 5d). Such indirect interactions between β-sheets A and B seem to play an important role in stabilizing the entire folding of the core fold.

Enhanced Stability of Ferredoxins. The core fold common to bacterial Fds adopts a quite simple $(\beta\alpha\beta)_2$ fold. The unfolding of the core fold may begin with dissociation of the two β-sheets. If the interaction between the β-sheets is strong, the unfolding of the core fold would be unlikely to occur. In this sense, the indirect interaction between β-sheets A and B may play an important role in enhancing the stability of bacterial Fd molecules. As mentioned above, ferredoxin molecules from *Sulfolobus* sp. strain 7, *A. vinelandii*, *B. thermoproteolyticus*, and their relatives are assumed to have acquired their own strategies for indirect interaction between the β-sheets in the course of the evolutionary process. In addition to the zinc ligation and the N-terminal extension, the *Sulfolobus* Fd seems to utilize the insertion in order to enhance the stability of the two β-sheets. In the *Sulfolobus* Fd, the loop region ranging from Thr 65 to Glu 72 (eight residues) is inserted between strands β5 and β6 in antiparallel β-sheet B. The inserted loop interacts with the loop between strand β4 and α-helix α2 in the core fold and with the loop between strands β2 and β3 in the N-terminal extension, respectively, through a hydrogen bond. The role of insertion in stabilization of bacterial Fds has not been clarified yet. However, the structure of *Sulfolobus* Fd shows that the insertion as well as the extension could take part in the indirect interaction between β-sheets A and B. Therefore, thermoacidophilic archaeal Fds may acquire thermostability by the novel zinc ligation, the formation of the larger β-sheet and the inserted loop interaction between the N-terminal extension and the core fold, as observed in the *Sulfolobus* Fd, which are conserved in the archaeal Fds. Further biochemical and biophysical studies on the roles of the zinc ion as well as the N-terminal extension and the inserted loop in thermoacidophilic archaeal Fds might lead to elucidation of the role of metal ions in protein thermostability.

Other strategies for enhancing the stability of β-sheets A and B may be utilized in bacterial Fds. Recently, the secondary structure of [3Fe-4S] monocluster ferredoxin from *Pyrococcus furiosus*, the hyperthermophilic archaeon which grows optimally at 100 °C, was determined by solution ^{1}H NMR (Teng et al., 1994). In the ferredoxin, a β-strand is formed instead of the loop between the C-terminal strand of the β-sheet B and the second long helix, and is located to the side of the N-terminal β-strand to make a triple-stranded antiparallel β-sheet A instead of the usual double-stranded β-sheet. Consequently, the β-sheets, A and B, may interact directly or indirectly through a short connection. The increase in the secondary structure content and the direct or indirect interaction between the β-sheets, A and B, may result in the formation of the ferredoxin molecule which possesses hyperthermostability.

In the course of evolution, different organisms have adapted to different environments; archaea have evolved special adaptation mechanisms to adapt to extreme environments where other organisms cannot live. It is interesting to investigate their adaptation mechanisms on the molecular level using ferredoxins for an example. Since ferredoxins may adopt various kinds of strategies to acquire enhanced stability as described previously, it does not seem so easy to propose a general mechanism for stabilizing the ferredoxin molecules. In thermoacidophilic archaeal Fds, however, the indirect interaction between β-sheets A and B through the zinc ligation, the N-terminal extension, and the insertion may play an important role in enhancing the stability of the protein molecules against denaturation under extreme environmental conditions.

ACKNOWLEDGMENT

We are deeply indebted to Dr. Toshio Iwasaki, Nippon Medical School, for his invaluable help in the material preparation and his helpful discussion.

REFERENCES

Adman, E. T., Sieker, L. C., & Jensen, L. H. (1976) *J. Biol. Chem. 251*, 3801−3806.

Breton, J. T., Duff, J. L. C., Butt, J. N., Armstrong, F. A., George, S. J., Pétillot, Y., Forest, E., Schäfer, G., & Thomson, A. J. (1995) *Eur. J. Biochem. 233*, 937−946.

Brünger, A. T. (1992a) *X-PLOR, Version 3.1: A system for Crystallography and NMR*, Yale University Press, New Haven, CT.

Brünger, A. T. (1992b) *Nature 355*, 472−474.

Bruschi, M., & Guerlesquin, F. (1988) *FEMS Microbiol. Rev. 54*, 155−176.

Cambillau, C. (1992) *Turbo-FRODO, Version 5.02*, Bio-Graphics, Marseille, France.
Duée, E. D., Fanchon, E., Vicat, J., Sieker, L. C., Meyer, J., & Moulis, J.-M. (1994) *J. Mol. Biol. 243*, 683−695.
Frolow, F., Harel, M., Sussman, J. L., Mevarech, M., & Shoham, M. (1996) *Nat. Struct. Biol. 3*, 452−458.
Fujii, T., Moriyama, H., Takenaka, A., Tanaka, N., Wakagi, T., & Oshima, T. (1991) *J. Biochem. (Tokyo) 110*, 472−473.
Fujii, T., Hata, Y., Wakagi, T., Tanaka, N., & Oshima, T. (1996) *Nat. Struct. Biol. 3*, 834−837.
Fukuyama, K., Nagahara, Y., Tsukihara, T., Katsube, Y., Hase, T., & Matsubara, H. (1988) *J. Mol. Biol. 199*, 183−193.
Fukuyama, K., Matsubara, H., Tsukihara, T., & Katsube, Y. (1989) *J. Mol. Biol. 199*, 183−193.
Furey, W., & Swaminathan, S. (1990) *Am. Crystallogr. Assoc. Annu. Mtg. Program Abstr. 18*, 73.
Iwasaki, T., Wakagi, T., Isogai, Y., Tanaka, K., Iizuka, T., & Oshima, T. (1994) *J. Biol. Chem. 269*, 29444−29450.
Iwasaki, T., Wakagi, T., & Oshima, T. (1995) *J. Biol. Chem. 270*, 17878−17883.
Kerscher, L., Nowitzki, S., & Oesterhelt, D. (1982) *Eur. J. Biochem. 128*, 223−230.
Kissinger, C. R., Sieker, L. C., Adman, E. T., & Jensen, J. H. (1991) *J. Mol. Biol. 219*, 693−715.
Kitagawa, Y., Tanaka, N., Hata, Y., Kusunoki, M., Lee, G.-P., Katsube, Y., Asada, K., Aibara, S., & Morita, Y. (1991) *J. Biochem. (Tokyo) 109*, 477−485.
Knaff, D. B., & Hirasawa, M. (1991) *Biochim. Biophys. Acta 1056*, 93−125.
Kraulis, P. J. (1991) *J. Appl. Crystallogr. 24*, 946−950.
Laskowski, R. A. (1993) *J. Appl. Crystallogr. 26*, 283−291.
Lovejoy, B., Cleasby, A. M., Hassel, A., Longley, K., Luther, M. A., Weigl, D., McGeehan, G., McElroy, A. B., Drewry, D., Lambert, M. H., & Jordan, S. R. (1994) *Science 263*, 375−377.
Minami, Y., Wakabayashi, S., Wada, K., Matsubara, H., Kerscher, L., & Oesterhelt, D. (1985) *J. Biochem. 97*, 745−753.
Séry, A., Housset, D., Serre, L., Bonicel, J., Hatchikian, C., Frey, M., & Michel, R. (1994) *Biochemistry 33*, 15408−15417.
Spurlino, J. C., Smallwood, A. M., Carlton, D. D., Banks, T. M., Vavra, K. J., Johnson, J. S., Cook, E. R., Falvo, J., Wahl, R. C., Pulvino, T. A., Wendoloski, J. J., & Smith, D. L. (1994) *Proteins: Struct., Funct., Genet. 19*, 98−109.
Stout, C. D. (1989) *J. Mol. Biol. 205*, 545−555.
Tainer, J. A., Getzoff, E. D., Beem, K. M., Richardson, J. S., & Richardson, D. C. (1982) *J. Mol. Biol. 160*, 181−217.
Teixeira, M., Batista, R., Campos, A. P., Gomes, C., Mendes, J., Pacheco, L., Anemuller, S., & Hangen, W. R. (1995) *Eur. J. Biochem. 227*, 322−327.
Teng, Q., Zhou, Z. H., Smith, E. T., Busse, S. C., Howard, J. B., Adams, M. W. W., & La Mar, G. N. (1994) *Biochemistry 33*, 6316−6326.
Wakabayashi, S., Fujimoto, N., Wada, K., Matsubara, H., Kersher, L., & Oesterhelt, D. (1983) *FEBS Lett. 162*, 21−24.
Wakagi, T., & Oshima, T. (1985) *Biochim. Biophys. Acta 817*, 33−41.
Wakagi, T., Fujii, T., & Oshima, T. (1996) *Biochem. Biophys. Res. Commun. 225*, 489−493.
Wang, B.-C. (1985) *Methods Enzymol. 115*, 90−117.
Woese, C. R., Kandler, O., & Wheelis, M. L. (1990) *Proc. Natl. Acad. Sci. U.S.A. 87*, 4576−4579.

BI961966J